# Predicting the Occurrence of Dynamic Transformation and Rolling Mill Loads Drops by Hot Torsion and Compression Testing

**John J. Jonas**[*]**, Chiradeep Ghosh, Xavier Quelennec, Vladimir V. Basabe**

Materials Engineering, McGill University, 3610 University St., Montreal, H3A 2B2, Canada

**Abstract**   Flow curves were determined in hot compression and hot torsion at a series of temperatures on eight C steels of increasing C concentration. The critical strains for the initiation of dynamic transformation (DT) as well as of dynamic recrystallization were determined by the double differentiation method. It is shown that dynamic transformation is initiated well before dynamic recrystallization under industrial conditions of rolling. The mean flow stresses (MFS's) pertaining to each experimental condition were then calculated from the flow curves by integration. These are plotted against inverse absolute temperature in the form of Boratto diagrams. The stress drop temperatures, normally defined as the upper critical temperature applicable to rolling $A_{r3}$*, were determined from these diagrams. These are shown to be about 40°C above the paraequilibrium and about 20-30℃ above the orthoequilibrium upper critical transformation temperatures. This type of behavior is ascribed to the occurrence of dynamic transformation during deformation. The general characteristics of the dynamic transformation of austenite to ferrite are reviewed. It is suggested that some of the unexpectedly low rolling loads, as well as the load drops that have been reported to take place above the $Ae_3$ temperature in strip mills, may be attributable to this phenomenon.

**Keywords**   Rolling Load, Mean Flow Stress, Dynamic Transformation, Dynamic Recrystallization, Critical Strain, Mechanical Testing

## 1. Introduction

The dynamic transformation (DT) of austenite to ferrite during rolling above the $Ae_3$ was first demonstrated by Yada and co-workers in the 1980's[1,2]. They were able to produce this kind of transformation as much as 166°C above the orthoequilibrium $Ae_3$. On holding after deformation, the DT ferrite was shown to re-transform to austenite, as required by equilibrium thermodynamics. Later, the occurrence of this phenomenon was verified by in-situ x-ray methods[3] as well as by laser dilatometry[4,5] and considerable modeling work has also been carried out[6,7]. More recently, the double differentiation method has been employed to determine the critical strains for DT[8,9]. These have been shown to be well below the critical strains required for the initiation of dynamic recrystallization, so that DT is generally underway well before DRX under the usual conditions of industrial rolling.

Although DT is generally initiated during finish rolling, it does not produce readily detectable effects for a number of

* Corresponding author:
john.jonas@mcgill.ca (John J. Jonas)

reasons. One is that the grains produced in this way are less than a micron in size and so are not readily observable using optical microscopy[10-15]. Another is that the rate of production of DT ferrite is quite low, ½ to 1% volume fraction per 1% strain[16], so that its initiation does not produce dramatic effects or sudden decreases in rolling load. However, because DT ferrite is softer than the austenite from which it has formed (at a given temperature), at the stage in rolling where significant volume fractions of DT ferrite have formed, they can have a measurable softening influence on the load. This is an effect that can be detected under appropriate conditions.

One way of predicting the occurrence and magnitude of the load drops due to DT is by carrying out hot compression and hot torsion experiments at the appropriate temperatures and then calculating the mean flow stress (MFS) by integration of the area under the curve. Such calculations can also be used to determine the effect of the accumulated strain below the $T_{nr}$ on the magnitude of the load drop. Experiments of this type are described below and it is shown that load drops of 10 to 50 MPa can be readily produced in this way. It therefore appears that one of the possible causes of unexpected reductions in rolling load in the austenite phase field as well as rolling loads that are lower than predicted in the absence of strain accumulation may well be

dynamic transformation. The calculations also explain why the values of the dynamic upper critical $Ar_3^*$ temperature derived using the Boratto[17] method can actually be higher than the equilibrium $Ae_3$ temperature.

# 2. Experimental Procedure

## 2.1. Materials

The flow behaviors of an ultralow 0.019%C, a 0.11%C-0.038%Nb microalloyed, and a 0.22%C-0.045%Nb steel were determined by means of hot compression testing. A further five steels, containing 0.06%C, 0.09%C-0.036%Nb, 0.21%C, 0.45%C, and 0.79%C were tested in hot torsion. Their detailed compositions and equilibrium transformation temperatures are presented in Table 1.

## 2.2. Test Procedure

The hot compression tests were carried out on an MTS test frame with the aid of a Research Incorporated radiation furnace and superalloy tooling. The TestStar software was employed for test programming and data acquisition and conversion. Details of the heating and cooling procedure followed are given in Refs. 18-20. The torsion tests were performed on an MTS-based hydraulic torsion machine, again using a Research Incorporated radiation furnace and superalloy tooling. Test programming and data acquisition and conversion were again accomplished using the TestStar software. Details regarding the austenite conditioning as well as the heating, cooling and quench schedule are provided in Refs. 10-15. Metallographic examinations of the quenched samples were carried out on a Philips XL-30 FE-SEM.

**Table 1.**    Chemical composition (wt %) and $Ae_3$ equilibrium transformation temperatures (°C)

| Steel | Composition (wt%) | $Ae_3$(℃) Orthoequilibrium | $Ae_3$(℃) Paraequilibrium |
|---|---|---|---|
| 1 | 0.019 C; 0.2 Si; 1.5 Mn; 0.017 Ti; 0.008 S; 0.005 P; 0.04 Al; 0.0089 N; 0.0005 B | 872 | 860 |
| 2 | 0.11 C; 0.26 Si; 1.1 Mn; 0.038 Nb; 0.003 S; 0.004 P; 0.03 Al; 0.003 N | 848 | 836 |
| 3 | 0.22 C; 1.56 Si; 1.56 Mn; 0.045 Nb; 0.017 Ti; 0.004 S; 0.006 P; 0.031 Al; 0.004 N | 860 | 850 |
| 4 | 0.06 C; 0.01 Si; 0.30 Mn | 877 | 870 |
| 5 | 0.09 C; 0.02 Si; 1.30 Mn; 0.036 Nb | 836 | 820 |
| 6 | 0.21 C; 0.24 Si; 1.30 Mn | 822 | 808 |
| 7 | 0.45 C; 0.24 Si; 0.70 Mn | 772 | 753 |
| 8 | 0.79 C; 0.24 Si; 0.65 Mn | 733 | 709 |

# 3. Results

## 3.1. Flow Curves

Some typical flow curves determined in compression are presented in Fig. 1. In the ultralow C steel, Fig. 1a), flow softening took place under all the experimental conditions, while in the Nb-modified plain C steel, Fig. 1b), there was net work hardening at the lower temperatures and flow softening at the higher temperatures. In the Nb-modified TRIP steel, the flow stress nearly saturates at the lowest temperature, while there is clear evidence of flow softening, usually attributed to dynamic recrystallization (DRX) at the higher temperatures. Some typical flow curves determined in torsion are illustrated in Fig. 2. Only the low C (0.06%C) steel exhibits the conventional 'single peak' behavior, while the four remaining steels display work hardening, leading to saturation in three of the steels.
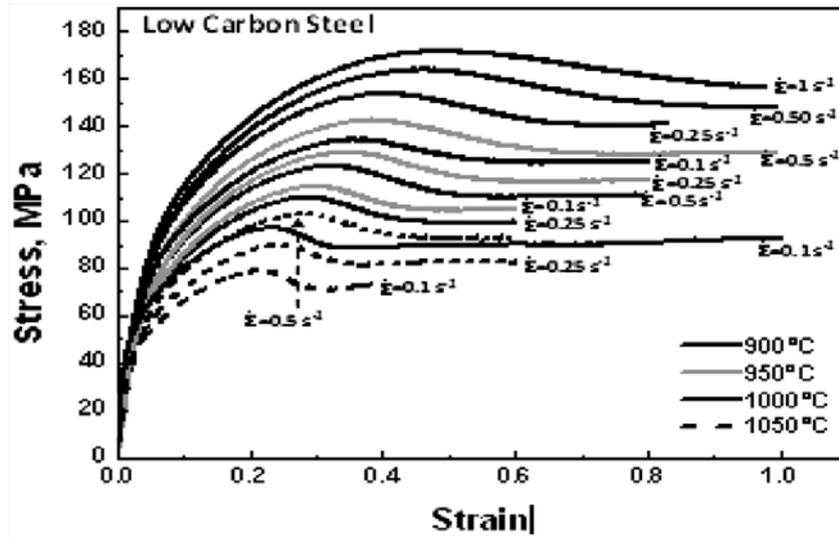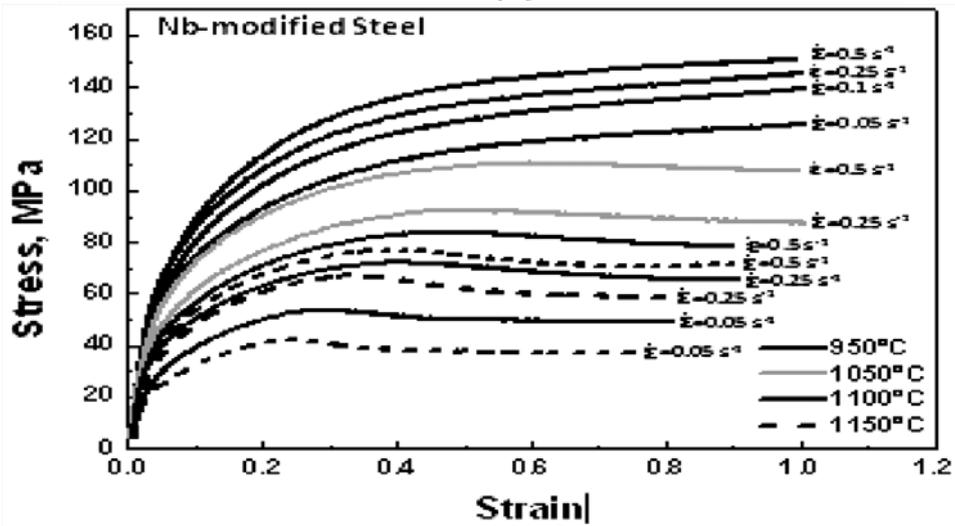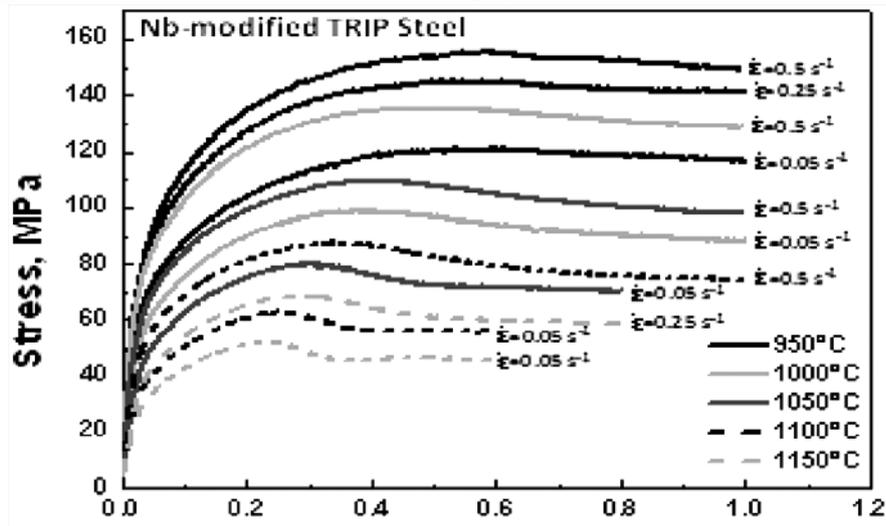
**Figure 1.** Hot compression flow curves determined on the: a) 0.019%C ultralow C; b) 0.11%C Nb-modified; and c) Nb- modified TRIP steels[19]
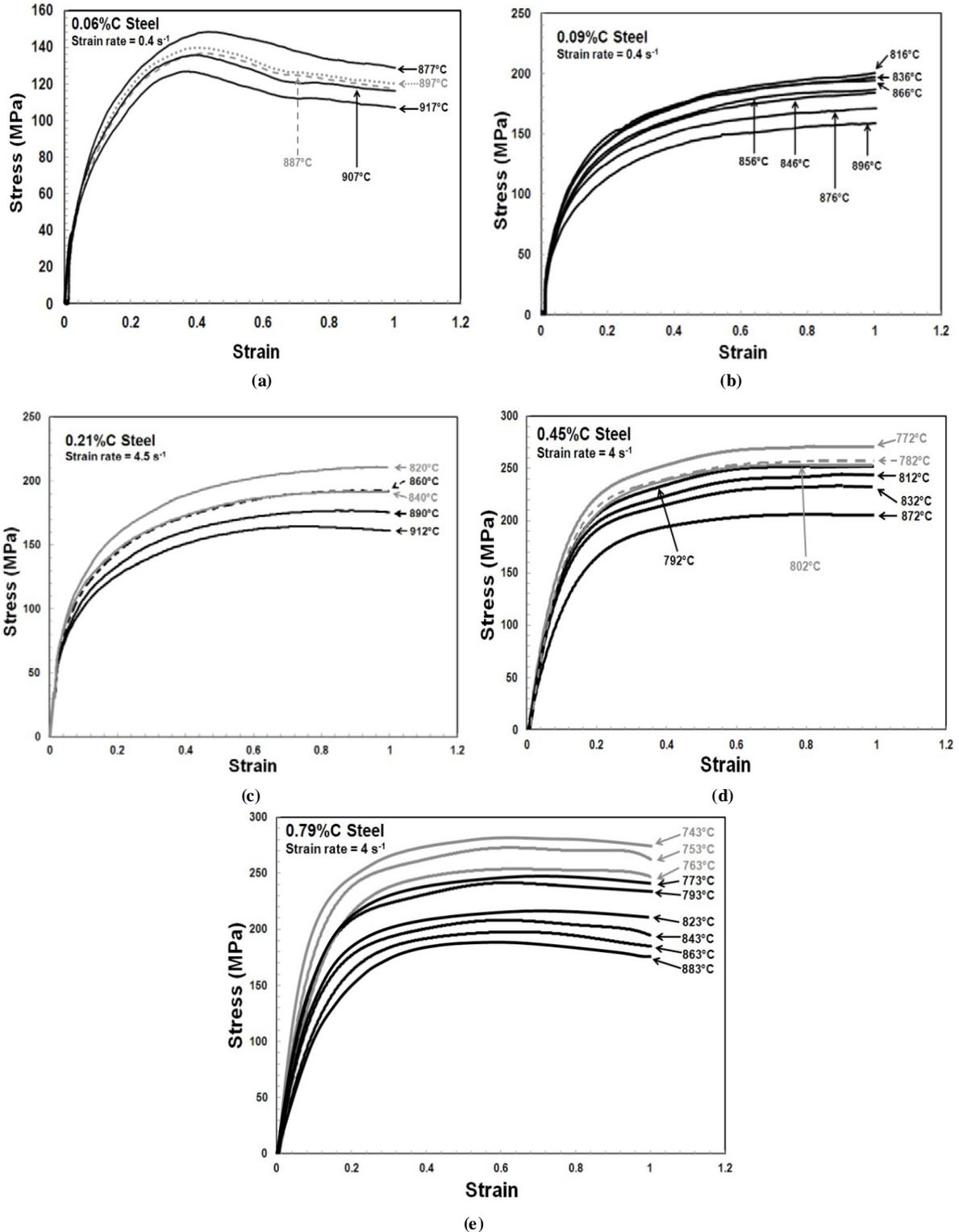
**Figure 2.** Hot torsion flow curves determined on the: a) 0.06%C[10]; b) 0.09%C-0.036%Nb[11]; c) 0.21%C[15]; d) 0.45%C[16] and e) 0.79%C[15] steels

### 3.2. Critical Strains

The double derivative procedure[21] was employed In order to determine the critical strains for the initiation of dynamic transformation (DT) as well as of DRX. This required the fitting of polynomials to the rising portion of each stress-strain curve. Polynomials of order 8 to 10 were used, as described in more detail in Ref. 22. Examples of the second-derivative plots determined on the 0.09%C-0.036% Nb steel are provided in Fig. 3, where $\theta$ is the slope of the stress-strain curve (first derivative) and $\partial\theta/\partial\sigma$ is the second derivative. Here it can be seen that there are two local minima on each plot, the first of which is associated with the initiation of DT and the second with the start of DRX. Similar results were obtained on the other steels[15].

The critical strains determined on four of the steels tested in torsion are illustrated in Fig. 4. Here it can be seen that the critical strains for the initiation of DT are quite low (about 0.1 to 0.25) and relatively insensitive to temperature and strain rate. They are always lower than those associated with DRX. The latter decrease with increasing temperature and decreasing strain rate in the manner normally associated with DRX[23]. The DT critical strains are in good agreement with the metallographic observations of ferrite formation during testing[10-15]. Similar results were obtained on the materials tested in compression[22], although the compression critical strains were always somewhat lower than those determined in torsion under comparable conditions.

### 3.3. Mean Flow Stresses

The mean flow stresses (MFS values) were determined from the flow curves by simple integration. These calculations were carried out using the Excel™ and Origin™ software programs. The results obtained were then plotted against inverse absolute temperature following the Boratto[17] procedure. The dependences observed are shown in Fig. 5 for the five steels tested in torsion.
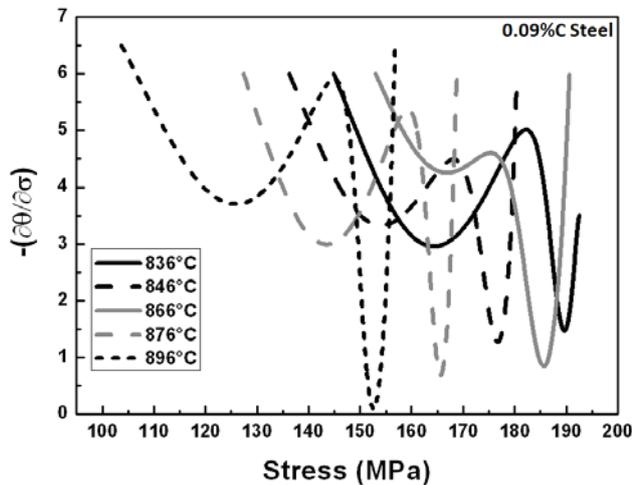


**Figure 3.** -(∂θ/∂σ) vs. σ plots derived from the flow curves of the 0.09%C-0.036%Nb steel[15]

# 4. Discussion

### 4.1. Mean Flow Stresses

Several features of these plots are of interest. First of all, it should be noted that all of the plots exhibit an $Ar_3^*$, i.e. a point at which the MFS suddenly drops, even though the temperature is *decreasing*, so that the MFS is expected to rise. This is because the ferrite being formed by DT is softer than austenite at the temperature of interest. Of particular interest is the observation that in every case, the drop temperature *is well above* the equilibrium upper critical $Ae_3$ temperature normally associated with phase transformation. Both the orthoequilibrium as well as paraequilibrium temperatures are indicated on the diagrams, from which it can be seen that the

dynamic $Ar_3^*$'s are something like 20-40 degrees above the ortho $Ae_3$ and as much as 30-60 degrees above the para $Ae_3$.
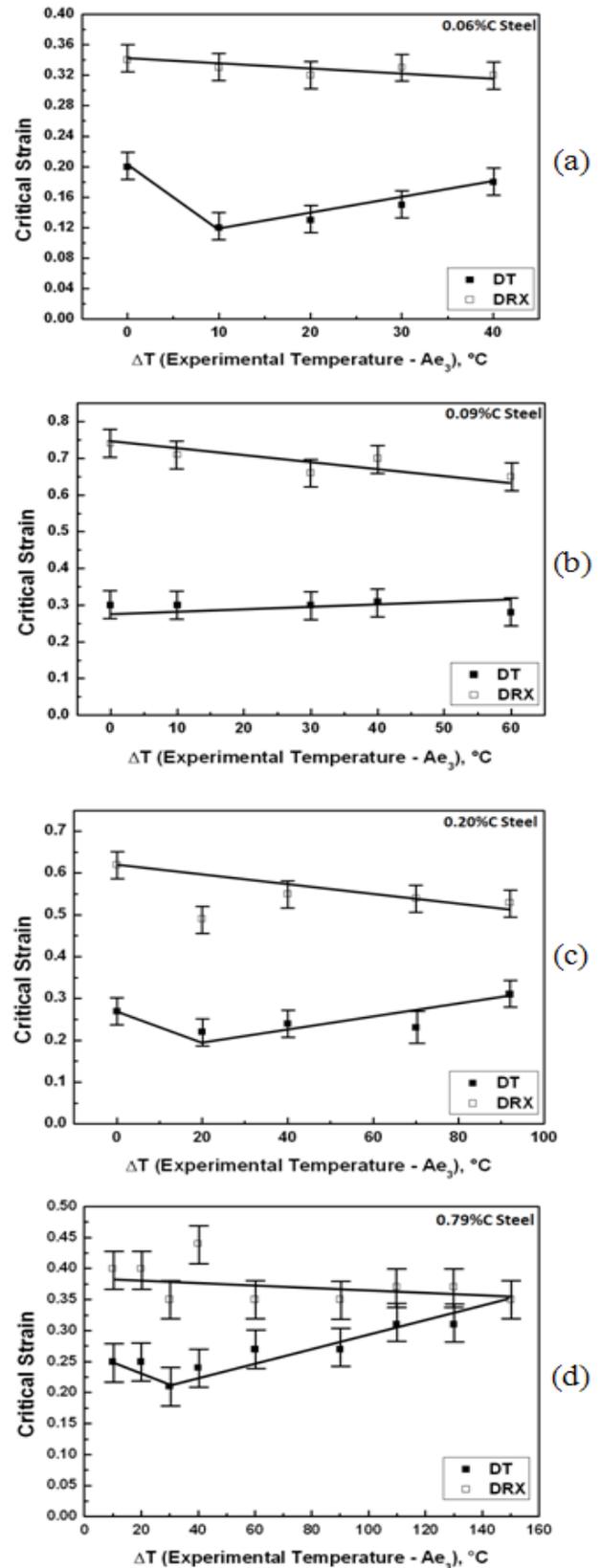


**Figure 4.** Critical strain determined by means of torsion testing: a) 0.06%C steel; b) 0.09%C steel; c) 0.21%C steel; and d) 0.79%C steel[15]

This unusual behavior can be attributed to the considerable increase in free energy of the austenite associated with straining[24]. The dislocations introduced raise the free energy of the deformed austenite to well above that of the undeformed ferrite, so that the effective transformation temperature can be increased by as much as 100-150 degrees. However, such DT ferrite forms quite slowly during deformation, being limited to about ½ to 1% volume fraction per 1% strain. Thus, even though DT ferrite begins to be formed well above the Ae$_3$, considerable strain must be accumulated before the volume fraction transformed is sufficient to produce a noticeable load drop[16].
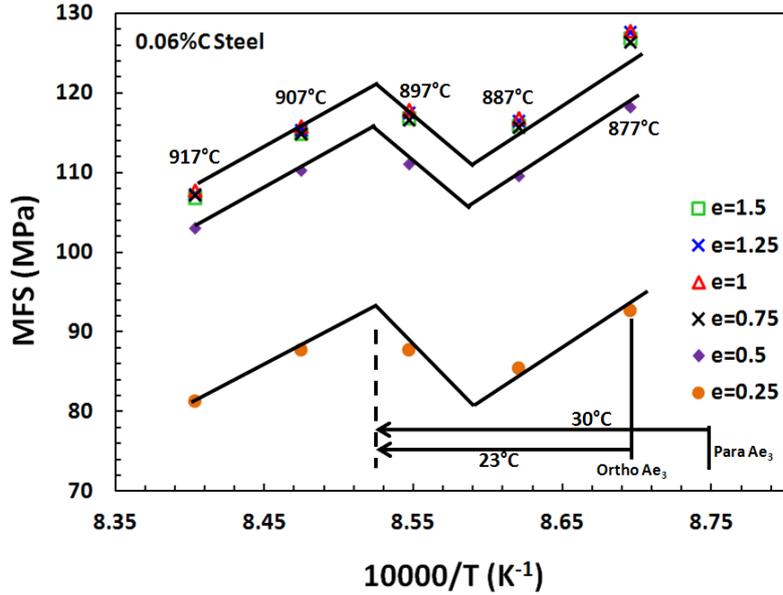


(a)
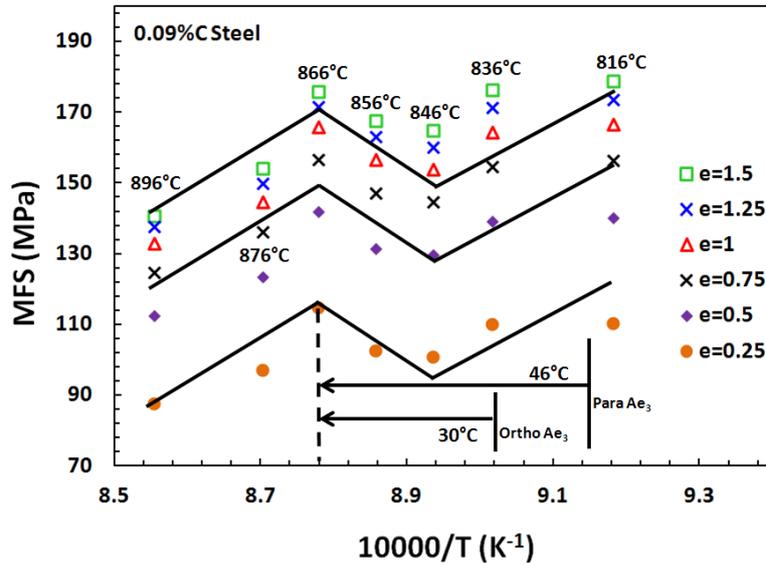


(b)
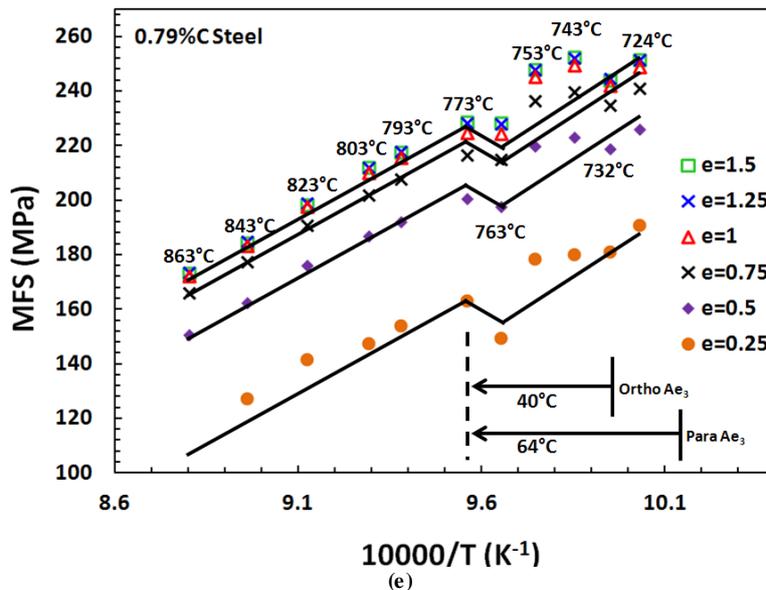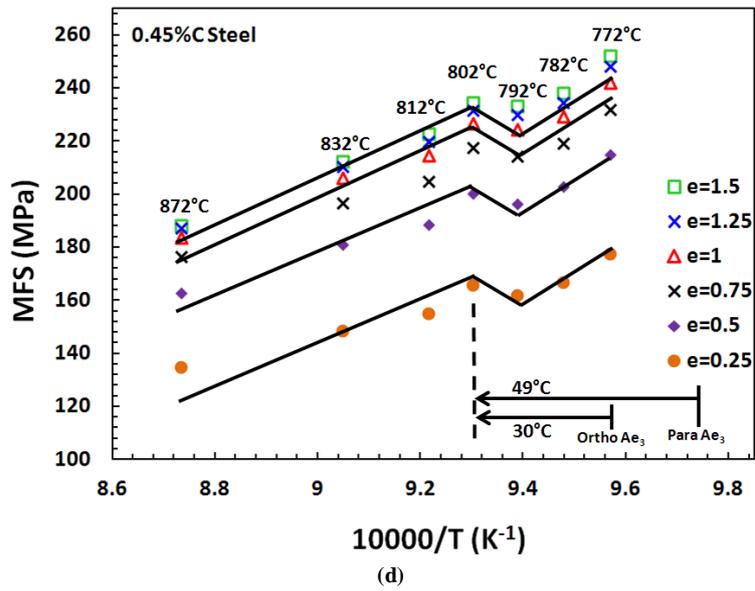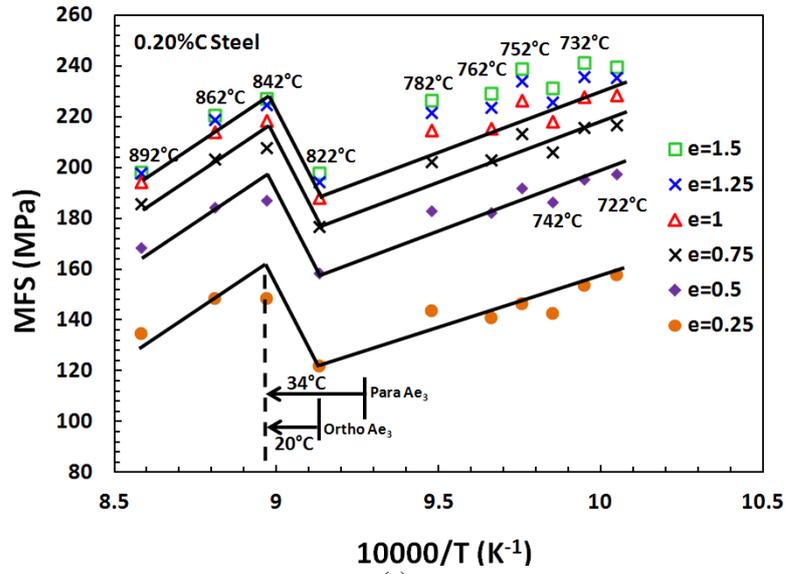
**Figure 5.** Mean flow stresses (MFS's) determined from the torsion testing flow curves

Another feature of interest concerns the effect of accumulated strain on the stress drop behavior. First of all, it appears that increasing the strain does not affect the stress drop *temperature* or Ar$_3$*, at least as can be determined from the fairly large temperature intervals employed here. It can also be seen that, while the *amount* of the stress drop increases slightly with accumulated strain, the *percentage* drop is nearly constant in each material over the strain range investigated. The percentage drops appear to decrease with increasing C concentration, ranging from about 35% for the 0.06% C steel, to 22%, 19%, 5%, and 6% for the 0.09% C, 0.21% C, 0.45% C, and 0.79% C steels, respectively.

From a practical point of view, there are several important conclusions to be drawn from MFS diagrams such as those of Fig. 5. The first is that the effective Ar$_3$*'s determined from laboratory measurements and interpreted using Boratto diagrams can frequently be *higher than* the Ae$_3$'s determined from the chemical composition using ThermoCalc. The second is that, due to DT, rolling loads can frequently be unexpectedly *lower* than estimates based on the increasing flow stress behavior of austenite when cooled down to the conventional Ae$_3$. This is because appreciable volume fractions of the softer ferrite can be present at a given temperature even though the presence of such ferrite is not called for by the conventional phase diagram. Finally, the presence of a dynamic Ar$_3$* that is higher than the Ae$_3$ has the practical effect of decreasing the expected temperature interval over which pancaking strains can be applied during controlled rolling.

### 4.2. Critical Strains and Softening Mechanisms

The conventional 'single peak' austenite flow curves of Fig. 1a) and 2a) are usually associated with the occurrence of DRX; their iconic shapes are thus generally attributed to the motion of the recrystallizing austenite grain boundaries, which remove dislocations and cause flow softening. However, it is clear from the critical strains presented in Fig. 4 that *two* flow softening mechanisms are acting concurrently during the high temperature deformation of austenite (in addition to dynamic recovery). That is, that the flow softening of austenite is actually caused by dynamic transformation as well as by dynamic recrystallization. This effect of DT has not been recognized to date for a number of reasons: i) one is that the DT ferrite plates produced in this way are so fine (under a micron in size) that they are not readily observable by optical microscopy; ii) the second is that the polygonal grains resulting from the coalescence and growth of the plates are usually considered to have formed *statically*, i.e. during cooling to room temperature (and not *dynamically*); and iii) finally the rate of formation of such DT ferrite is quite low, so that it does not generally produce any dramatic effects.

## 5. Conclusions

1. Hot torsion and hot compression testing can be used to determine the critical strains for dynamic transformation as well as the mean flow stresses applicable to rolling.

2. The double differentiation method is readily adaptable to calculating the critical strain for DT.

3. The DT critical strains are well below those associated with the initiation of DRX and indicate that, up to fairly high temperatures, the flow softening taking place during the high temperature deformation of austenite is generally caused by these two flow softening mechanisms occurring simultaneously.

4. As a result of DT, the Ar$_3$* temperatures determined by the Boratto method are generally *higher than* the ortho or para equilibrium Ae$_3$'s.

5. Ferrite formation at such high temperatures is brought about by the increase in free energy of the deformed austenite associated with the presence of the dislocations introduced by straining.

## ACKNOWLEDGEMENTS

## REFERENCES

[1]  H. Yada, Y. Matsumura and T. Senuma, Proc. of the Int. Conf. on Martensitic Transformation, JIM, 1986, pp. 515 - 520.

[2]  H. Yada, Y. Matsumura and T. Senuma, Proc. 1st Conf. on Physical Metallurgy of Thermomechanical Processing of Steels and Other Metals (THERMEC-88), Ed. I. Tamura, ISIJ, Tokyo, 1988, pp. 200 - 207.

[3]  H. Yada, C. M. Li and H. Yamagata, ISIJ International, Vol. 40, 2000, p. 200.

[4]  Y. Chen and Q. Chen, J Iron Steel Research International, Vol. 10, 2003, p. 46.

[5]  X. Sun, H. Luo, H. Dong, Q. Liu and Y. Weng, ISIJ International, Vol. 48, 2008, p. 994.

[6]  M. Tong, J. Ni, Y. Zhang, D. Li and Y. Li, Metall. Mater. Trans. A, Vol. 35, 2004, p. 1565.

[7]  N. Xiao, M. Tong Y. Lan, D. Li and Y. Li, Acta Mater., Vol. 54, 2006, p. 1265.

[8]  X. Sun, H. Luo, H. Dong, Q. Liu and Y. Weng, ISIJ International, Vol. 48, 2008, p. 994.

[9]  J. K. Choi, D. H. Seo, J. S. Lee, K. K. Um and W. Y. Choo, ISIJ International, Vol. 43, 2003, p. 746.

[10]  V. V. Basabe, J. J. Jonas and H. Mahjoubi, ISIJ International, Vol. 51, 2011, p. 612.

[11]  V. V. Basabe and J. J. Jonas, ISIJ International, Vol. 50, 2010, p. 1185.

[12]  V. V. Basabe, J. J. Jonas and C. Ghosh, Adv. Mater. Res., Vol.

409, 2012, p. 829.

[13] V. V. Basabe, J. J. Jonas and C. Ghosh, Steel Res. International, submitted.

[14] C. Ghosh, V. V. Basabe and J. J. Jonas, ISIJ International, submitted.

[15] C. Ghosh, V. V. Basabe and J. J. Jonas, Steel Res. International, submitted.

[16] J. J. Jonas, C. Ghosh and V. V. Basabe, Steel Res. International, In press.

[17] F. Boratto, R. Barbosa, S. Yue and J.J. Jonas, Proc. of the 1st Conf. on Physical Metallurgy of Thermomechanical Processing of Steels and Other Metals (THERMEC-88), Ed. I. Tamura I, ISIJ, Tokyo, 1988, pp. 383 - 390.

[18] J. J. Jonas, X. Quelennec and Lan Jiang, Materials Science Forum, Vol. 715-716, 2012, p. 81.

[19] X. Quelennec and J. J. Jonas, ISIJ International, Vol. 52, 2012, p. 1145.

[20] X. Quelennec, N. Bozzolo, J. J. Jonas and R. Loge, ISIJ International, Vol. 51, 2011, p. 945.

[21] E. Poliak and J. J. Jonas, Acta Mater., Vol. 44, 1996, p. 127.

[22] J. J. Jonas, C. Ghosh, X. Quelennec and V. V. Basabe, ISIJ International, in press.

[23] T. Sakai and J. J. Jonas, Acta Metall., Vol. 32, 1984, p. 189.

[24] C. Ghosh, V. V. Basabe, J. J. Jonas, Y. M. Kim, I. H. Jung and S. Yue: Acta Mater., submitted.